Int J Clin Exp Pathol 2017;10(2):1455-1465
www.ijcep.com /ISSN:1936-2625/IJCEP0041428

Original Article

Inhibition of RIPK1 expression and facilitation of TRAIL-induced hepatocellular carcinoma cell apoptosis by miR-141

Minjie Shang, Defei Hong, Zhiming Hu, Chengwu Zhang, Weiding Wu

Department of Hepatopancreaticobiliary Surgery & Laparoscopic Minimally Invasive Surgery, Zhejiang Provincial People's Hospital, Hangzhou, Zhejiang, P. R. China

Received October 9, 2016; Accepted November 25, 2016; Epub February 1, 2017; Published February 15, 2017

Abstract: Receptor-interacting protein kinase 1 (RIPK1) activates NF-κB and facilitates cell survival under tumor necrosis factor related apoptosis inducing ligand (TRAIL) induction, thus negatively regulating cell apoptosis but leaving detailed mechanism unclear. Previous study showed depressed expression of microRNA (miR)-141 in hepatocellular carcinoma (HCC) patients. Bioinformatics analysis showed satisfactory targeted relationship between miR-141 and 3'-UTR of RIPK1. This study thus investigated the role of miR-141 and RIPK1 expressional dysregulation in HCC cell apoptosis. Rat HCC model was generated to test miR-141 and RIPK1 expression. HCC patients were recruited to compare expression levels between HCC and adjacent tissues. Dual luciferase reporter assay substantiated targeting relationship between miR-141 and RIPK1. Cultured HepG2 cells were treated with 80 ng/mL TRAIL, miR-141 mimic and/or si-RIPK1. Caspase-3 activity was measured in addition to flow cytometry for cell apoptosis, plus CCK-8 assay for proliferative activity. Western blot was used to test transcriptional activity of RIPK1 and NF-κB proteins. Rat HCC tissue had lower miR-141 and higher RIPK1 expression, as those in HCC patients. MiR-141 targeted 3'-UTR of RIPK1 and inhibited its expression. TRAIL up-regulated RIKP1 expression in HepG2 cells. Elevation of miR-141 and/or silencing RIPK1 inhibited TRAIL-induced NF-κB transcriptional activation, weakened cell proliferative activity, potentiated caspase-3 activity and facilitated cell apoptosis. MiR-141 targeted and inhibited RIPK1, inhibited TRAIL-induced NF-κB transcriptional activation in HepG2 cells, and facilitated TRAIL-induced caspase-3 activation and apoptosis.

Keywords: MicroRNA-141, receptor-interacting protein kinase 1, hepatocellular carcinoma, HepG2, cell apoptosis

Introduction

Primary liver cancer is one of the most common malignant tumor in clinics, as its incidence is listed on 5th of all cancers, and mortality as 3rd one, only next to pulmonary carcinoma and gastric cancer [1]. Hepatocellular carcinoma (HCC) is one major pathological subtype of primary liver cancer, as it occupies about 80%~90% [2]. More than 600 thousand people died from HCC, with over 110 thousand in China, occupying 18.3% of world counts [3]. Tumor necrosis factor related apoptosis inducing ligand (TRAIL) selectively induced tumor cell apoptosis and prevent killing effects on normal cells, thus becoming new generation of anti-tumor drugs with promising insights [4]. Amounts of evidences showed drug-resistance against TRAIL-induced cell apoptosis in almost all liver cancer cell lines [5-7]. Receptor-interacting protein kinase 1 (RIPK1) is one serine/threonine protein kinase with molecular weight at 74KD, containing death structural domain, kinase structural domain and intermediate structural domain, and plays an important role in regulating cell apoptosis and survival [8]. RIPK1 is one negatively regulatory molecular for transducing apoptotic signals in TRAIL-activated death-inducing signaling complex (DISC) [9]. Previous findings showed that intermediate structural domain of RPIK1 can activate nuclear factor kappa B (NF-κB) and facilitate cell proliferation and survival, indicating the facilitation on tumor pathogenesis by RIPK1-induced NF-κB activation and cell proliferation [10]. Abnormally elevated RIPK1 expres-

sion has been shown to be related with pathogenesis of various tumors such as melanoma [11], gallbladder carcinoma [12] and breast cancer [13]. Up-regulation of RIPK1 has also been demonstrated to be related with TRAIL-induced decreased sensitivity of TRAIL-induced apoptosis in HCC cells [7, 14]. However, detailed mechanism of abnormally elevated RIPK1 expression is still unknown yet. MicroRNA is one type of non-coding single stranded RNA with 22~25 nucleotide length in eukaryotes, and can negatively regulate gene expression via targeted degradation of mRNA or inhibiting translation of target gene mRNA, thus participating in biological processes including cell proliferation, apoptosis and differentiation, leading to widespread interests on its expression and function abnormality in tumor pathogenesis [15]. Previous studies showed significantly lowered miR-141 expression in HCC tumor tissues [16, 17], thus indicating possible tumor-suppressor role of miR-141 in HCC pathogenesis. Bioinformatics analysis revealed satisfactory targeted complementary relationship between miR-141 and 3'-untranslated region (3'-UTR) of RIPK1. This study thus investigated the role of miR-141 and RIPK1 expressional dysregulation in affecting HCC cell apoptosis and pathogenesis.

Materials and methods

Reagent and materials

Male SD rats (8~10 weeks age, body weight 220~240 g) were purchased from Medical Laboratory Animal Center, Zhejiang, China. Diethylnitrosamine (DEN) was provided by Pesticide Institute, Agriculture Science Academy of Sichuan, China. Human liver cancer cell line HepG2 and normal human hepatocytes L02 were purchased from ATCC (US); DMEM culture medium, fetal bovine serum (FBS) and penicillin-streptomycin were purchased from Gibco (US). Recombinant human TRAIL factor was purchased from Peprotech (US). Reverse transcription kit PrimeScipt RT reagent Kit and SYBR Green dye were purchased from TaKaRa (Japan). Cell-Light EdU cell proliferation assay kit was purchased from Ruibo Bio (China). Mouse anti-human cleaved caspase-3 was purchased from CST (US). Mouse anti-human RIPK1 and rabbit anti-human p-p65 antibody was purchased from Abcam (US). Mouse anti-human DR4 and DR5 antibody was purchased from Santa Cruz (US). Annexin V/PI apoptotic kit was purchased from Yusheng (China). Caspase-3 activity kit was purchased from Beyotime (China). Dual-Luciferase Reporter assay system and pGL3-promoter were purchased from Promega (US).

Clinical information

A total of 56 HCC patients who were diagnosed in Zhejiang Provincial People's Hospital from October 2015 to April 2016 were recruited. Tumor tissues and adjacent tissue samples (≥5 cm from tumor edge) were collected during surgery. There were 30 males and 26 females, aging between 34 and 61 years (average age = 45.7 ± 14.9 years). Sample collection was approved by the ethical committee of Zhejiang Provincial People's Hospital, and has obtained written consents from patients.

Induced liver cancer model

Using 40 SD rats, 0.25% DEN solution was given by gastric intubation (10 mg/kg body weight weekly), leaving freely drinkable 0.025% DEN water solution. After 6 months, a total of 25 SD rats had liver cancer (62.5% induction rate). Another 25 SD rats with normal feeding were recruited as control group. Animals were sacrificed to remove tumor or normal liver tissues, which were fixed in 4% paraformaldehyde, followed by routine dehydration, paraffin embedding and sectioning. HE staining was then performed to observe tissue morphology.

In vivo EdU labelling

EdU labelling was used to test *in vivo* cell proliferation inside tissues. In brief, 72 h before sacrificing, animals received EdU dye in PBS via intraperitoneal injection (5 mg/Kg body weigth). 72 h later, liver tissues were collected for preparing paraffin-based sections (5 μm). Tissue sections were rinsed in xylene, dehydrated in gradient ethanol, and rinsed in glycine 2 mg/mL for 10 min. After incubation in 0.5% Triton X-100 in PBS for 10 min, tissue sections were rinsed in PBS for 10 min, followed by adding 100 μL 1 × Apollo staining reaction buffer for 30 min dark incubation at room temperature. After rinsing in 0.5% Triton X-100 in PBS for 2~3 times (10 min each) and methanol rinsing (5 min), microscopic observation was performed.

HepG2 cell culture and TRAIL treatment

Human HCC cell line HepG2 and normal liver cell L02 were cultured high-glucose DMEM containing 10% FBS and 1% penicillin-streptomycin, and were incubated in 37°C chamber with 5% CO_2, with medium changing every 2 days. Experiment was performed when reaching 60%~80% confluence. Cells were collected after treating with 0, 20, 40 and 80 ng/mL TRAIL for 24 h to test all indexes.

CCK-8 assay for cell proliferative activity

Cultured cells were seeded into 96-well plate at 8000 per well density. After attached growth for 24 h, cells were treated with 0, 20, 40 and 80 ng/mL TRAIL for 48 h. Original medium was removed, followed by adding 100 μL fresh medium containing 10 μL CCK-8 reagent, and incubation at 37°C for 4 h. Absorbance (A) values at 450 nm were then measured by a microplate reader. Six parallel samples were performed in each treatment group. Relative activity of cells was calculated by $(A_{\text{drug treatment group}} - A_{\text{Blank control}})/A_{\text{Control group}} \times 100\%$.

Construction of luciferase reporter assay plasmid

Using HEK293 genome as the template, full length fragment of 3'-UTR of RIPK1 gene was amplified. PCR products were purified from agarose gel, and were ligated into pGL-3M luciferase reporter plasmid after XbaI/NotI dual digestion. Recombinant plasmid was then used to transform DH5α competent cells. Positive clones with primary screening were selected for sequencing. Those plasmids with correct sequence were used for further cell transfection and following experiments.

Luciferase reporter assay

Lipofectamine 2000 was used to transfect HEK293 cells with 400 ng pGL3-RIPK1-3'UTR plasmid, 25 nmol miR-141 mimic (or miR-21 negative control), and 25 ng controlled plasmid pRL-TK. After 4~6 h transfection, Opti-MEM medium was discarded, with the replacement of normal DMEM medium containing 10% FBS and 1% streptomycin-penicillin. After 48 h continuous incubation, dual-luciferase assay was performed. In brief, cells were washed twice in PBS, with the addition of 100 μL PLB lysis buffer. With vortex at room temperature for 20 min, the mixture was centrifuged at 300 rpm for 5 min. 20 μL cell lysate was mixed with 100 μL LAR II. Fluorescent value I was measured in a microplate reader. The enzymatic reaction was stopped in 100 μL Stop & Glo, followed by quantification of fluorescent value II. The relative expression level of reporter gene was calculated as the ratio of fluorescent value I/fluorescent value II.

HepG2 cell transfection

Cultured HepG2 cells treated with 80 ng/mL were divided into 6 groups: non-treated group, mimic NC control, miR-141 mimic group, si-NC group, si-RIPK1 group, and miR-141 + si-RIPK1 group. Lipofectamine 2000 was used to transfect oligonucleotide fragments into HepG2 cells cultured in serum-and antibiotic-free medium. After 6 h, DMEM medium containing 10% FBS and 1% streptomycin-penicillin was added for 48 h continuous culture in further experiments. Oligonucleotide sequences were: mimic NC, 5'-UUCUCCGAACGUGUCACGUTT-3'; miR-141 mimic, 5'-UAACACUGUCUGGUAAAGAUGG-3'; si-RIPK1 sense, 5'-CCACUAGUCUGACGGAUAAUU-3'; si-RIPK1 anti-sense, 5'-UUAUCCGUCAGACUAUGGUAA-3; si-NC sense, 5'-UUCUCCGAACGUGUCACGUUU-3'; si-NC anti-sense, 5'-ACGUGACACGUUCGGAGAAUU-3'.

qRT-PCR assay for gene expression

Total RNA was extracted from cells by Trizol method. In brief, cells were lysed by 1 mL Trizol, and RNA were extracted by 200 μL chloroform. The supernatant was saved. RNA was precipitated by 1 mL isopropanol, followed by twice rinsing in 1 ml 70% ethanol in centrifugation. RNA precipitation was solved in DEPC treated water. cDNA was synthesized in a 10 μL system including 1 μg total RNA, 2 μL RT buffer (5 ×), 0.5 μL oligo dT + random primer mix, 0.5 μL RT enzyme mix, 0.5 μL RNase inhibito, and ddH_2O. The reaction conditions were: 37°C for 15 min, followed by 98°C 5 min. cDNA products were kept at -20°C fridge. Using cDNA as the template, PCR amplification was performed under the direction of TaqDNA polymerase using primers (miR-141P_{RT}: 5'-GTCGTATGTTGGCGTGTCGTGGAGTCGGCAATTGCACTGGATACCTCTCCATAA-3'; miR-141P_F: 5'-GCCTGTAGCTTTTCCTACT-3'; miR-141P_R: 5'-CACGGCGGTTCGTCGAGT-3'; U6P_F: 5'-ATTGGAACGATACA-

GAGAAGATT-3'; U6P_R: 5'-GGAACGCTTCACGAATTTG-3'; RIPK1P_F: 5'-GCACTGTTGTGACTCGTTGG-3'; RIPK1P_R: 5'-GACACCCGACCATACTTTCAG-3'; β-actinP_F: 5'-GAACCCTAAGGCCAAC-3'; β-actinP_R: 5'-TGTCA CGCAC GATTT CC-3'; In a PCR system with 10 μL total volume, we added 4.5 μL 2 × SYBR Green Mixture, 1.0 μL of forward/reverse primer (at 2.5 μm/L), 1 μL cDNA, and 3.0 μL ddH_2O. PCR conditions were: 95°C for 15 s, 60°C for 30 s and 74°C for 30 s. The reaction was performed on Bio-Rad CFX96 fluorescent quantitative PCR cycler for 40 cycles to collect fluorescent data.

Western blot

RIPA buffer was used to lyse cells, which were incubated on ice for 20 min, followed by 12000 g centrifugation for 20 min. 50 μg protein samples were separated by 8% SDS-PAGE (50 V for 250 min), and were transferred to PVDF membrane (300 mA for 100 min). The membrane was blocked in 5% defatted milk powder for 1 h, followed by primary antibody (anti-RIPK1 at 1:300, anti-p-p65 at 1:200, anti-cleaved caspase-3 at 1:200 or anti-beta-actin at 1:800) incubation at 4°C overnight. By PBST washing (5 min × 3 times), HRP-labelled secondary antibody (1:10000 for both anti-mouse and anti-rabbit) was added for 1 h incubation. After PBST rinsing for three times (5 min each), ECL reagent was added for 2 min dark incubation. The membrane was then exposure in dark. Quantity One image analysis software (BioRad, US) was used to analyze relative grey density of bands.

Caspase-3 activity assay

Standard dilutions of 0, 10, 20, 50, 100 and 200 μM pNA were prepared from 10 mM stock. Absorbance values at 405 nm wavelength were measured by a microplate reader to plot a standard curve with pNA concentration against A405 value. Attached cells were digested in trypsin, and were collected into culture medium for 4°C centrifugation for 5 min at 600 g. Supernatant was carefully removed and washed out by PBS. 100 μL lysis buffer was added for every 2 × 10^6 cells. Cells were lysed at 4°C for 15 min, and were centrifuged at 18000 g with 4°C for 10 min. Supernatants were saved for further use. Ac-DEVD-pNA was placed on ice, mixed with buffer and test samples, with 10 μL Ac-DEVD-pNA. The mixture was incubated at 37°C for 2 h. A405 value was measured when color changed significantly.

Flow cytometry for cell apoptosis

Cells were digested by trypsin and were collected by 1000 rpm centrifugation for 5 min. Cells were then washed in pre-cold PBS twice by centrifugation. 100 μL 1 × Binding Buffer was used to re-suspend cells. The mixture was added with 5 μL Annexin V-FITC and 5 μL PI staining solution. The mixture was incubated in dark for 10 min, with the addition of 400 μL 1 × Binidng Buffer, and was immediately loaded for online testing.

Statistical analysis

SPSS18.0 software was used for data analysis. Measurement data were presented as mean ± standard deviation (SD). Student t test was used to compare measurement data between groups. A statistical significance was defined when $P<0.05$.

Results

Elevated RIPK1 and decreased miR-141 expressions in HCC model animals

After DEN treatment by gastric intubation for 6 months on SD rats, the induction rate of HCC was 62.5% (25/40). HE staining showed normal cell morphology and size inside normal rat liver tissues, which had complete and regularly arranged hepatic lobules. In model group, however, normal hepatic lobular structure disappeared, with enlarged cell volume and irregular arrangement inconsistent with peripheral tissues (**Figure 1A**). EdU labelling results showed more positive cells in HCC model tissues compared to normal rats, indicating active proliferation in HCC tumor tissues (**Figure 1B**). qRT-PCR results showed significantly depressed miR-141 expression level in HCC model compared to normal animals, whilst RIPK1 mRNA expression level was significantly higher (**Figure 1C**). Western blot revealed remarkably elevated RIPK1 protein expression in HCC tissues compared to normal liver tissues (**Figure 1D**).

Elevated RIPK1 and decreased miR-141 expressions in HCC patient tumor tissues

qRT-PCR showed significantly lowered miR-141 expression and elevated RIPK1 mRNA expres-

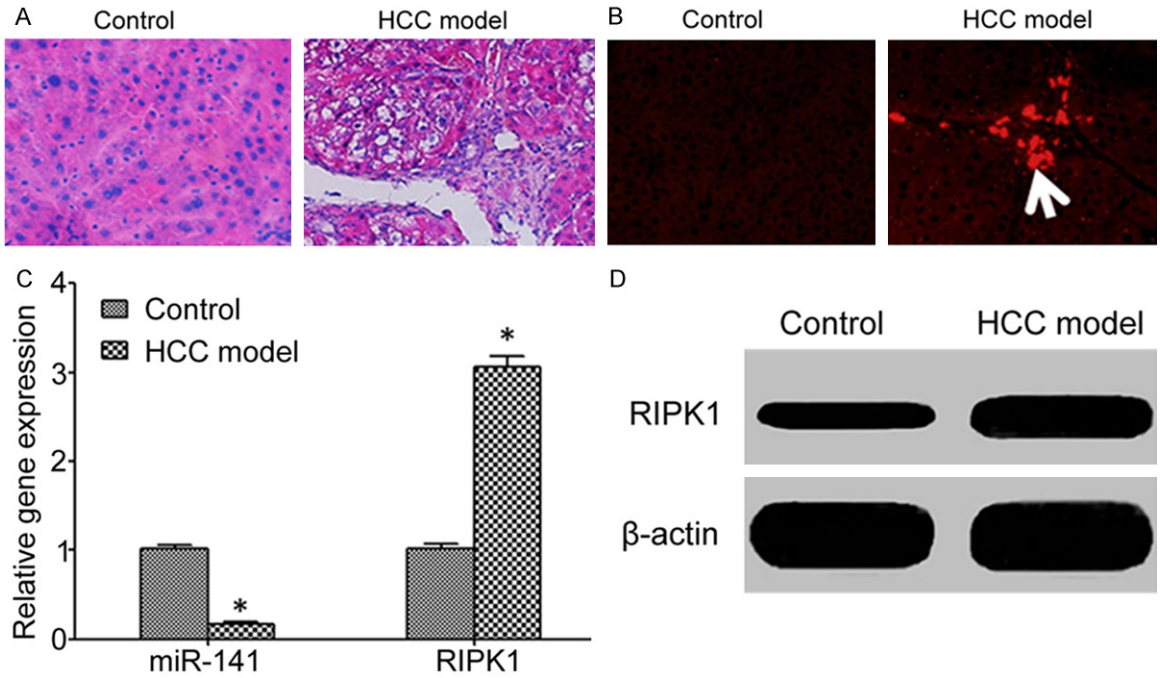

Figure 1. Elevated RIPK1 and lowered miR-141 expressions in HCC tissues. A: HE staining for liver tissue morphology change; B: EdU labelling for cell proliferation; C: qRT-PCR detecting miR-141 and RIPK1 gene expression; D: Western blot assay for RIPK1 protein expression. *, P<0.05 compared to controlled normal rats.

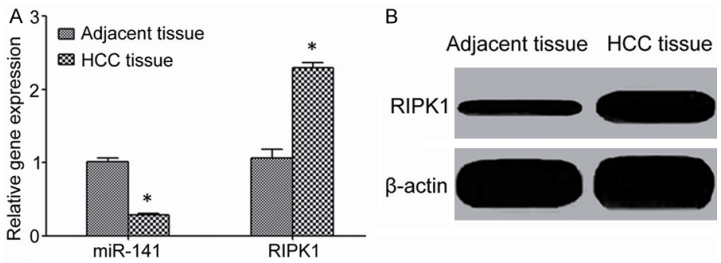

Figure 2. Elevated RIPK1 and lowered miR-141 expressions in HCC patient tumor tissues. A: qRT-PCR detecting miR-141 and RIPK1 gene expression; B: Western blot assay for RIPK1 protein expression. *, P<0.05 compared to tumor adjacent tissues.

sions in tumor tissues of HCC patients compared to those in adjacent tissues (**Figure 2A**). Western blot results showed remarkably higher RIPK1 protein expression in tumor tissues than adjacent tissues (**Figure 2B**). Spearman analysis showed significantly negative correlation between miR-141 and RIPK1 mRNA level ($r = -0.716$, $P = 0.024$), indicating targeted regulation between miR-141 and RIPK1.

miR-141 in HepG2 cell line inhibited RIPK1 expression

CCK-8 assay showed inhibition of HepG2 cell proliferation by different TRAIL treatment to certain extents but with weak effects, suggesting resistance of HepG2 cells against TRAIL (**Figure 3A**). Flow cytometry results showed no significant increase of TRAIL-induced apoptosis with higher dosage, indicating resistance against TRAIL-induced cell apoptosis of HepG2 cells (**Figure 3B**). Compared to normal human hepatocellular cell L02, miR-141 expression and basal apoptotic rate of HepG2 cell were significantly lower (**Figure 3C**) whilst RIPK1 expression level was elevated (**Figure 3D** and **3E**). Moreover, high level of TRAIL (80 ng/mL) also elevated RIPK1 expression in HepG2 cells (**Figure 3E**). Results showed miR-141 down-regulation and RIPK1 up-regulation may also play a role in antagonizing HCC apoptosis. Bioinformatics analysis showed satisfactory targeting relationship between miR-141 and 3'-UTR of RIPK1 mRNA (**Figure 3F**). Dual-luciferase reporter gene assay showed remarkably decreased relative luciferase activity by miR-141 up-regulation (**Figure 3G**), demonstrating that miR-141 could target 3'-UTR of RIPK1 mRNA to regulate its expression. After trans-

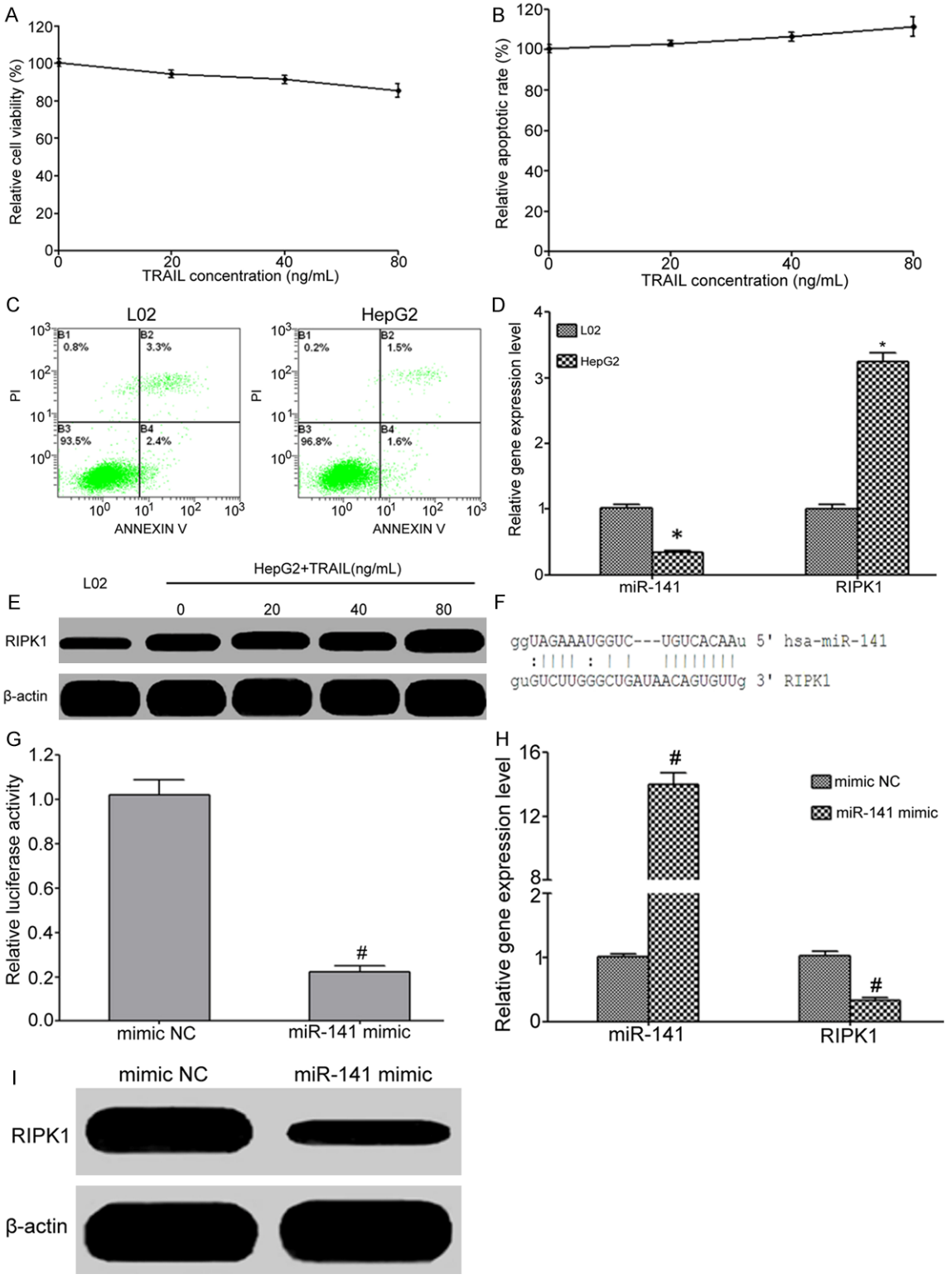

Figure 3. MiR-141 inhibited RIPK1 expression in HepG2 cells. A: CCK-8 for cell proliferative activity; B: Flow cytometry for cell apoptotic rate; C: Flow cytometry for basal apoptosis of L02 and HepG2 cells; D: qRT-PCR for gene expression in L02 and HepG2 cells; E: Western blotting for RIPK1 protein expression in L02 and HepG2 cells; F: miR-215 targeting on 3'-UTR of RIPK1 mRNA; G: Dual-luciferase reporter gene assay; H: qRT-PCR for miR-141 and RIPK1 gene expression; I: Western blot for RIPK1 protein expression. *, P<0.05 compared to L02 cells; #, P<0.05 compared to mimic NC group.

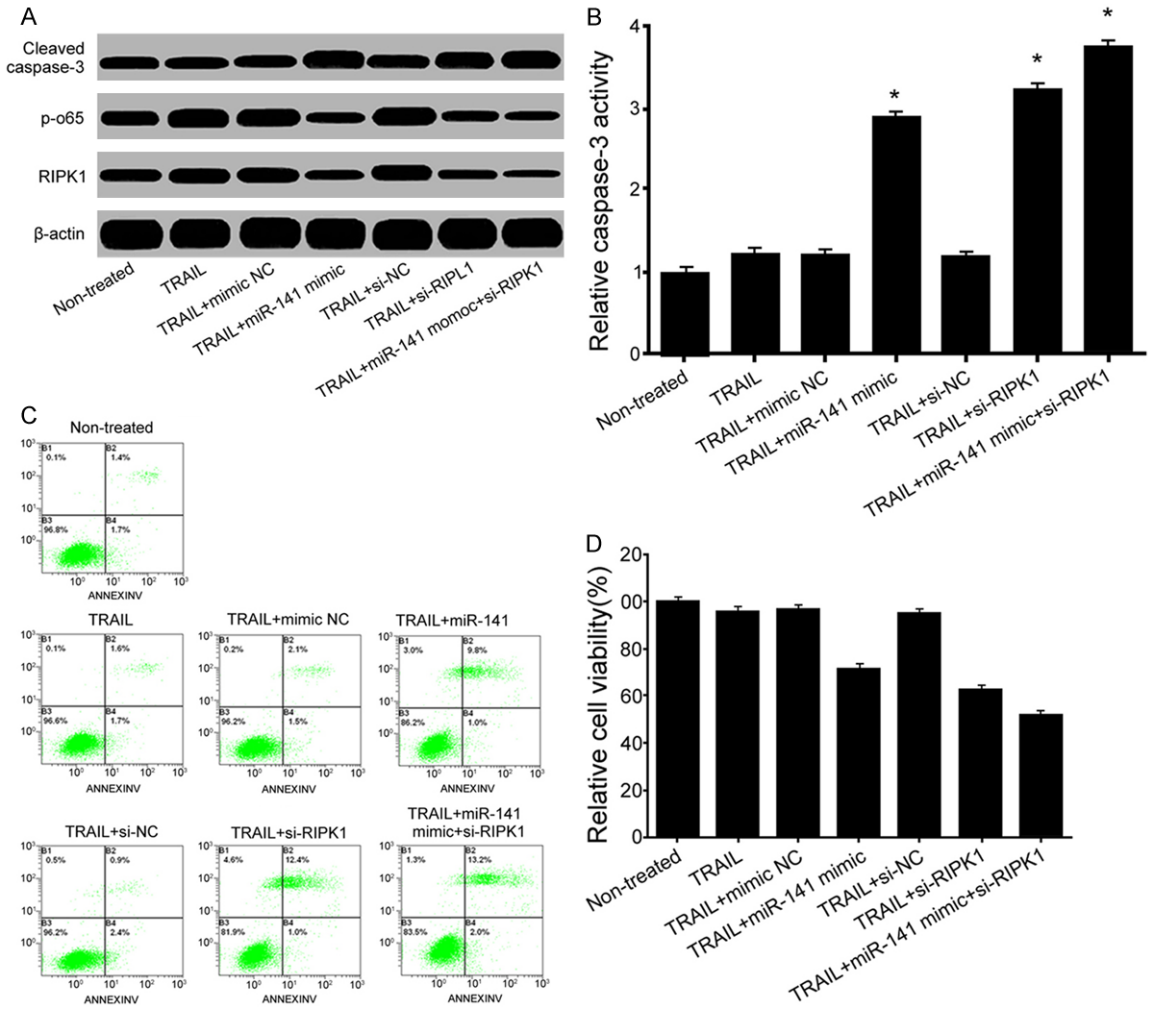

Figure 4. MiR-141 inhibited RIPK1 and weakened TRAIL-induced NF-κB activation and facilitated HepG2 cell apoptosis. A: Western blot for protein expression; B: Spectrometry for caspase-3 activity; C: Flow cytometry for cell apoptosis; D: CCK-8 assay for cell proliferative activity. *, P<0.05 compared to single TRAIL treatment group.

fecting miR-141 mimic in HepG2 cells for 48 h, mRNA and protein expression of RIPK1 were significantly decreased, further confirming targeted inhibition of miR-141 on RIPK1 expression (**Figure 3H** and **3I**).

miR-141 inhibited RIPK1 and suppressed TRAIL-induced NF-κB activation for facilitating HepG2 cell apoptosis

Western blotting results showed high basal level of RIPK1 in HepG2 cells. TRAIL treatment significantly increased RIPK1 expression in HepG2 cells. TRAIL treatment also elevated p-p65 protein expression, indicating potentiation of NF-κB transcriptional activity. No significantly facilitating effect, however, was observed in caspase-3 enzymatic activity (**Figure 4A** and **4B**), nor did the inhibition on cell proliferation or induction on cell apoptosis (**Figure 4C** and **4D**). Transfection of miR-141 mimic and/or si-RIPK1, RIPK1 expression in HepG2 cells was significantly depressed (**Figure 4A**) while NF-κB transcriptional activity was remarkably decreased (**Figure 4A**), accompanied with potentiated caspase-3 activity (**Figure 4A** and **4B**), enhanced cell apoptosis (**Figure 4C**) and weakened proliferative activity (**Figure 4D**), indicating that RIPK1 up-regulation enhanced TRAIL-induced NF-κB transcriptional activity, and played a role in decreased TRAIL-induced apoptotic sensitivity in HepG2 cells. On the other hand, miR-141 down-regulation is one reason for elevated RIPK1 expression, the potentiation of miR-141 expression, therefore,

depressed RIPK1 expression and facilitated TRAIL-induced HCC cell apoptosis.

Discussion

HCC is one of common malignant tumors in China, with both incidence and mortality at frontline of cancers [18]. China is one popular region for hepatitis B, which makes HCC incidence higher. Among over 600 thousand newly discovered HCC patients worldwide, China occupies about 340 thousand (more than 55%), thus severely affecting people health [19, 20]. Young people are high risk population of HCC. Due to high malignancy, rapid progression and lack of early sensitive index, most patients are already at late or terminal phase when first diagnosis, making treatment more difficult and unfavorable treatment efficiency or prognosis [21]. Surgical resection is currently major method treating HCC. Post-op metastasis and recurrence, however, severely limits clinical treatment efficiency and patient's survival. Although treatment combining chemotherapy, radiotherapy, biotherapy and immune therapy had significant improvements, 1-year and 2-year survival rates were only 42.8% and 38.8%, respectively [20], with 5-year survival rate of HCC lower than 7% [22]. TRAIL in one important membrane of tumor necrosis factor (TNF) superfamily, and is one newly discovered targeted death receptor (DR) to induce endogenous cell apoptosis [23]. TRAIL can selectively function on tumor cells, transforming cells and viral infecting cells for inducing apoptosis, whilst had no significant toxicity or killing effects on normal cells [4]. TRAIL is now at phase II clinical trial, and has been recognized as the new generation of anti-tumor reagent for drawing increasing research interests [24]. Previous finding showed that although TRAIL could induce apoptosis of various tumor cells, almost all HCC cells showed low sensitivity for TRAIL-induced apoptosis, thus limiting its application in treating liver cancer. Such resistance against apoptosis severely affects TRAIL's treatment efficacy, and is also one important reason for post-op HCC metastasis and recurrence. The detailed mechanism of HCC for resistance against TRAIL-induced apoptosis, however, is still unclear [25, 26].

TRAIL can bind with death receptor 4 (DR4) or death receptor 5 (DR5) on membrane, further recruiting downstream signal molecules to form DR4/DR5-FADD-Procaspase-8 death inducing signaling complex (DISC), which facilitates self-cleavage of procaspase-8 to form apoptosis initiator caspase-8 with activity, and induce caspase cascade reaction to activate executor caspase-3, -6 and -7, finally leading to apoptosis [27]. RIPK1 is one negatively regulatory molecule for apoptotic signal transduction in TRAIL-activated DISC. Binding of TRAIL onto DR4 or DR5 recruits and forms DISC to initiate apoptosis. Moreover, DR4 or DR5 can also bind with RIP-1 via tumor necrosis factor receptor type 1-associated DEATH domain protein (TRADD) to activate NF-κB signal pathway. RIP-1 recruitment is critical for TRAIL-activated NF-κB transcriptional activity and facilitation of cell proliferation and survival [28], the latter of which induces resistance of cells against TRAIL-induced apoptosis, making cells having resistance against TRAIL to different extents [29], as one tumor facilitating factor during pathogenesis [10]. Previous study showed the role of abnormally elevated RIPK1 expression in occurrence of multiple tumors [11-13]. Elevated RIPK1 expression has also been demonstrated to be related with lower sensitivity of HCC cells against TRAIL-induced apoptosis [7, 14]. The detailed mechanism of abnormally elevated RIPK1 expression, however, is still unclear. Previous studies showed significantly depressed miR-141 in HCC tumor tissues, indicating possible tumor-inhibitor role of miR-141 in HCC pathogenesis. Bioinformatics analysis revealed satisfactory targeted complementary relationship between miR-141 and 3'-UTR of RIPK1. This study thus investigated if miR-141 and RIPK1 dysregulation played a role in affecting HCC cell apoptosis and pathogenesis.

Using DEN-induced liver cancer rat model, we found significantly elevated RIPK1 expression in HCC tissues compared to normal liver tissues, whilst miR-141 expression was significantly lower. Clinical samples showed consistent patterns, as HCC patients' tumor tissues had higher RIPK1 and lower miR-141 expression, indicating possible role of miR-141 down-regulation in up-regulating RIPK1 and facilitating liver cancer. Lou et al found that lower miR-141 expression facilitated tumor progression in HCC patients [16]. Lin et al showed significantly lower expression of tumor suppressor gene miR-141 in liver cancer tissues compared to adjacent tissues, whilst elevating miR-141

expression remarkably inhibited migration or invasion of liver cancer cells and facilitated their apoptosis [17]. This study observed significantly depressed miR-141 expression in HCC tumor tissues, as Lou et al [16] and Lin et al [17] reported. CCK-8 assay and flow cytometry results showed lower sensitivity of HepG2 HCC cells against TRAIL-induced cell apoptotic sensitivity, plus weak inhibitory effect of TRAIL on proliferation of HepG2 cells. Further assay showed remarkably lower miR-141 expression in HepG2 cells than L02 hepatocytes. High yields of basal RIPK1 and p-p65, plus elevated TRAIL can significantly up-regulated RIPK1 expression in addition to basal levels. Sun et al found that TRAIL treatment remarkably up-regulated RIPK1 expression and enhanced NF-κB transcriptional activity in HepG2 and Hep3B cells, but without significant apoptosis induced effects. This study largely agreed with these experiments. Dual-luciferase reporter gene assay showed significantly depressed relative luciferase activity by miR-141 mimic transfection, which can also down-regulate RIPK1 expression in HepG2 cells, demonstrating targeted regulation of RIPK1 by miR-141. Further analysis showed that up-regulation of miR-141 and/or silencing RIPK1 expression inhibited transcriptional activation of NF-κB by TRAIL in HepG2 cells, potentiated proliferative inhibition on HepG2 cells by TRAIL, and facilitated TRAIL-induced caspase-3 activation, thus inducing cell apoptosis. Sun et al showed siRNA interference of RIPK1 expression remarkably potentiated sensitivity of HepG2 cells on TRAIL-induced cell apoptosis [14]. Dong et al found elevated RIPK1 expression also caused drug resistance in apoptosis induced by other drugs in addition to TRAIL-induced ones [7]. Gong et al found that over-expression of RIPK1 or silencing can antagonize or facilitate Shikonin-induced HCC cell apoptosis, respectively. During liver cancer pathogenesis, miR-141 likely plays a tumor suppressor gene's role. Xue et al showed miR-141 could inhibit HCC cell proliferation and migration via targeting E2F3 [30, 31]. Wu et al showed weakened motility and migration of liver cancer cells by miR-141 targeting on ZEB2 [32]. Lin et al also revealed that miR-141 targeted HNF-3β, compromised proliferation and migration potency of tumor cells, and facilitated their apoptosis. This study revealed targeted inhibition on RIPK1 by miR-141, plus the role of HepG2 cells on TRAIL-induced cell apoptotic sensitivity. Abnormally elevated RIPK1 expression caused by miR-141 down-regulation might be one important reason for drug resistance of HCC cells against TRAIL.

Conclusion

MiR-141 was down-regulated in miR-141, whilst RIPK1 expression was elevated in liver cancer cells. miR-141 targeted and inhibited RIPK1, suppressed transcriptional activation of NF-κB by TRAIL in HepG2 cells, and facilitated TRAIL-induced caspase-3 activation and cell apoptosis.

Acknowledgements

Research supported by the Projects of medical and health program in Zhejiang Province (NO.2015KYB042) and the Projects of medical major science and technology in Zhejiang Province (NO.WKJ-ZJ-1602).

Disclosure of conflict of interest

None.

Address correspondence to: Dr. Defei Hong, Department of Hepatopancreaticobiliary Surgery & Laparoscopic Minimally Invasive Surgery, Zhejiang Provincial People's Hospital, 158 Shangtang Road, Hangzhou 310014, Zhejiang, P. R. China. Tel: +86-571-85893419; Fax: +86-571-85893419; E-mail: DefeiHong1518@163.com

References

[1] Wallace MC, Preen D, Jeffrey GP and Adams LA. The evolving epidemiology of hepatocellular carcinoma: a global perspective. Expert Rev Gastroenterol Hepatol 2015; 9: 765-79.

[2] Lafaro KJ, Demirjian AN and Pawlik TM. Epidemiology of hepatocellular carcinoma. Surg Oncol Clin N Am 2015; 24: 1-17.

[3] Park JW, Chen M, Colombo M, Roberts LR, Schwartz M, Chen PJ, Kudo M, Johnson P, Wagner S, Orsini LS and Sherman M. Global patterns of hepatocellular carcinoma management from diagnosis to death: the BRIDGE Study. Liver Int 2015; 35: 2155-66.

[4] Sophonnithiprasert T, Nilwarangkoon S, Nakamura Y and Watanapokasin R. Goniothalamin enhances TRAIL-induced apoptosis in colorectal cancer cells through DR5 upregulation and cFLIP downregulation. Int J Oncol 2015; 47: 2188-96.

[5] Fayyaz S, Yaylim I, Turan S, Kanwal S and Farooqi AA. Hepatocellular carcinoma: targeting of oncogenic signaling networks in TRAIL resistant cancer cells. Mol Biol Rep 2014; 41: 6909-17.
[6] Cheng CF, Lu IH, Tseng HW, Sun CY, Lin LT, Kuo ZK, Pan IH and Ko CH. Antitumor effect of periplocin in TRAIL-resistant human hepatocellular carcinoma cells through downregulation of IAPs. Evid Based Complement Alternat Med 2013; 2013: 958025.
[7] Dong B, Lv G, Wang Q, Wei F, Bellail AC, Hao C and Wang G. Targeting A20 enhances TRAIL-induced apoptosis in hepatocellular carcinoma cells. Biochem Biophys Res Commun 2012; 418: 433-8.
[8] Jin L, Chen J, Liu XY, Jiang CC and Zhang XD. The double life of RIPK1. Mol Cell Oncol 2016; 3: e1035690.
[9] Matsuda I, Matsuo K, Matsushita Y, Haruna Y, Niwa M and Kataoka T. The C-terminal domain of the long form of cellular FLICE-inhibitory protein (c-FLIPL) inhibits the interaction of the caspase 8 prodomain with the receptor-interacting protein 1 (RIP1) death domain and regulates caspase 8-dependent nuclear factor kappaB (NF-kappaB) activation. J Biol Chem 2014; 289: 3876-87.
[10] Zhang L, Dittmer MR, Blackwell K, Workman LM, Hostager B and Habelhah H. TRAIL activates JNK and NF-kappaB through RIP1-dependent and -independent pathways. Cell Signal 2015; 27: 306-14.
[11] Liu XY, Lai F, Yan XG, Jiang CC, Guo ST, Wang CY, Croft A, Tseng HY, Wilmott JS, Scolyer RA, Jin L and Zhang XD. RIP1 kinase is an oncogenic driver in melanoma. Cancer Res 2015; 75: 1736-48.
[12] Zhu G, Chen X, Wang X, Li X, Du Q, Hong H, Tang N, She F and Chen Y. Expression of the RIP-1 gene and its role in growth and invasion of human gallbladder carcinoma. Cell Physiol Biochem 2014; 34: 1152-65.
[13] Palacios C, Lopez-Perez AI and Lopez-Rivas A. Down-regulation of RIP expression by 17-dimethylaminoethylamino-17-demethoxygeldanamycin promotes TRAIL-induced apoptosis in breast tumor cells. Cancer Lett 2010; 287: 207-15.
[14] Sun J, Luo H, Nie W, Xu X, Miao X, Huang F, Wu H and Jin X. Protective effect of RIP and c-FLIP in preventing liver cancer cell apoptosis induced by TRAIL. Int J Clin Exp Pathol 2015; 8: 6519-25.
[15] Chen X, Fan S and Song E. Noncoding RNAs: new players in cancers. Adv Exp Med Biol 2016; 927: 1-47.
[16] Lou G, Dong X, Xia C, Ye B, Yan Q, Wu S, Yu Y, Liu F, Zheng M, Chen Z and Liu Y. Direct targeting sperm-associated antigen 9 by miR-141 influences hepatocellular carcinoma cell growth and metastasis via JNK pathway. J Exp Clin Cancer Res 2016; 35: 14.
[17] Lin L, Liang H, Wang Y, Yin X, Hu Y, Huang J, Ren T, Xu H, Zheng L and Chen X. microRNA-141 inhibits cell proliferation and invasion and promotes apoptosis by targeting hepatocyte nuclear factor-3beta in hepatocellular carcinoma cells. BMC Cancer 2014; 14: 879.
[18] Yao H, Bian X, Mao L, Zi X, Yan X and Qiu Y. Preoperative enteral nutritional support in patients undergoing hepatectomy for hepatocellular carcinoma: a strengthening the reporting of observational studies in epidemiology article. Medicine (Baltimore) 2015; 94: e2006.
[19] Tanaka M, Katayama F, Kato H, Tanaka H, Wang J, Qiao YL and Inoue M. Hepatitis B and C virus infection and hepatocellular carcinoma in China: a review of epidemiology and control measures. J Epidemiol 2011; 21: 401-16.
[20] Que J, Kuo HT, Lin LC, Lin KL, Lin CH, Lin YW and Yang CC. Clinical outcomes and prognostic factors of cyberknife stereotactic body radiation therapy for unresectable hepatocellular carcinoma. BMC Cancer 2016; 16: 451.
[21] Liu PH, Hsu CY, Hsia CY, Lee YH, Su CW, Huang YH, Lee FY, Lin HC and Huo TI. Prognosis of hepatocellular carcinoma: assessment of eleven staging systems. J Hepatol 2016; 64: 601-8.
[22] Su L, Zhou T, Zhang Z, Zhang X, Zhi X, Li C, Wang Q, Jia C, Shi W, Yue Y, Gao Y and Cheng B. Optimal staging system for predicting the prognosis of patients with hepatocellular carcinoma in China: a retrospective study. BMC Cancer 2016; 16: 424.
[23] Huang K, Zhang J, O'Neill KL, Gurumurthy CB, Quadros RM, Tu Y and Luo X. Cleavage by caspase 8 and mitochondrial membrane association activate the BH3-only protein bid during TRAIL-induced apoptosis. J Biol Chem 2016; 291: 11843-51.
[24] Bellail AC, Qi L, Mulligan P, Chhabra V and Hao C. TRAIL agonists on clinical trials for cancer therapy: the promises and the challenges. Rev Recent Clin Trials 2009; 4: 34-41.
[25] Shin EC, Seong YR, Kim CH, Kim H, Ahn YS, Kim K, Kim SJ, Hong SS and Park JH. Human hepatocellular carcinoma cells resist to TRAIL-induced apoptosis, and the resistance is abolished by cisplatin. Exp Mol Med 2002; 34: 114-22.
[26] Li J, Sun RR, Yu ZJ, Liang H, Shen S and Kan Q. Galectin-1 modulates the survival and tumor necrosis factor-related apoptosis-inducing ligand (TRAIL) sensitivity in human hepatocellular carcinoma cells. Cancer Biother Radiopharm 2015; 30: 336-41.

[27] Ramamurthy V, Yamniuk AP, Lawrence EJ, Yong W, Schneeweis LA, Cheng L, Murdock M, Corbett MJ, Doyle ML and Sheriff S. The structure of the death receptor 4-TNF-related apoptosis-inducing ligand (DR4-TRAIL) complex. Acta Crystallogr F Struct Biol Commun 2015; 71: 1273-81.
[28] Li H, Kobayashi M, Blonska M, You Y and Lin X. Ubiquitination of RIP is required for tumor necrosis factor alpha-induced NF-kappaB activation. J Biol Chem 2006; 281: 13636-43.
[29] Bellail AC, Tse MC, Song JH, Phuphanich S, Olson JJ, Sun SY and Hao C. DR5-mediated DISC controls caspase-8 cleavage and initiation of apoptosis in human glioblastomas. J Cell Mol Med 2010; 14: 1303-17.
[30] Xue J, Niu YF, Huang J, Peng G, Wang LX, Yang YH and Li YQ. miR-141 suppresses the growth and metastasis of HCC cells by targeting E2F3. Tumour Biol 2014; 35: 12103-7.
[31] Gong K and Li W. Shikonin, a Chinese plant-derived naphthoquinone, induces apoptosis in hepatocellular carcinoma cells through reactive oxygen species: A potential new treatment for hepatocellular carcinoma. Free Radic Biol Med 2011; 51: 2259-71.
[32] Wu SM, Ai HW, Zhang DY, Han XQ, Pan Q, Luo FL and Zhang XL. MiR-141 targets ZEB2 to suppress HCC progression. Tumour Biol 2014; 35: 9993-7.